Electron Transfer between the Quinones in the Photosynthetic Reaction Center and Its Coupling to Conformational Changes†

Björn Rabenstein, G. Matthias Ullmann,‡ and Ernst-Walter Knapp*

Institut für Chemie, Fachbereich Biologie, Chemie, Pharmazie, Freie Universität Berlin, Takustrasse 6, D-14195 Berlin, Germany

Received February 23, 2000; Revised Manuscript Received May 24, 2000

ABSTRACT: The electron transfer between the two quinones Q_A and Q_B in the bacterial photosynthetic reaction center (bRC) is coupled to a conformational rearrangement. Recently, the X-ray structures of the dark-adapted and light-exposed bRC from *Rhodobacter sphaeroides* were solved, and the conformational changes were characterized structurally. We computed the reaction free energy for the electron transfer from $Q_A^{\bullet-}$ to Q_B in the X-ray structures of the dark-adapted and light-exposed bRC from *Rb. sphaeroides*. The computation was done by applying an electrostatic model using the Poisson−Boltzmann equation and Monte Carlo sampling. We accounted for possible protonation changes of titratable groups upon electron transfer. According to our calculations, the reaction energy of the electron transfer from $Q_A^{\bullet-}$ to Q_B is +157 meV for the dark-adapted and −56 meV for the light-exposed X-ray structure; i.e., the electron transfer is energetically uphill for the dark-adapted structure and downhill for the light-exposed structure. A common interpretation of experimental results is that the electron transfer between $Q_A^{\bullet-}$ and Q_B is either gated or at least influenced by a conformational rearrangement: A conformation in which the electron transfer from $Q_A^{\bullet-}$ to Q_B is inactive, identified with the dark-adapted X-ray structure, changes into an electron-transfer active conformation, identified with the light-exposed X-ray structure. This interpretation agrees with our computational results if one assumes that the positive reaction energy for the dark-adapted X-ray structure effectively prevents the electron transfer. We found that the strongly coupled pair of titratable groups Glu-L212 and Asp-L213 binds about one proton in the dark-adapted X-ray structure, where the electron is mainly localized at Q_A, and about two protons in the light-exposed structure, where the electron is mainly localized at Q_B. This finding agrees with recent experimental and theoretical studies. We compare the present results for the bRC from *Rb. sphaeroides* to our recent studies on the bRC from *Rhodopseudomonas viridis*. We discuss possible mechanisms for the gated electron transfer from $Q_A^{\bullet-}$ to Q_B and relate them to theoretical and experimental results.

Electron-transfer reactions in proteins can be coupled to structural rearrangements (*1*−*3*). In these cases, the electron-transfer rate does not depend on the reaction free energy, which contradicts the classical Marcus theory (*4*, *5*). Such electron-transfer reactions are gated or at least influenced by processes that are not the actual redox event, for example, by conformational transitions or protonation reactions. The electron transfer between $Q_A^{\bullet-}$ and Q_B in the bacterial photosynthetic reaction center (bRC)[1] is apparently such a gated reaction (*2*).

The bRC is a pigment−protein complex in the membrane of purple bacteria. It converts light energy into electrochemical energy by coupling photoinduced electron transfer to proton uptake from cytoplasm. The X-ray structures of the bRC from *Rhodopseudomonas (Rps.) viridis* (*6*−*9*) and from *Rhodobacter (Rb.) sphaeroides* (*10*−*14*) enabled a more detailed understanding of the various functional processes in the bRC. The present work considers the light-exposed and dark-adapted X-ray structures of the bRC of *Rb. sphaeroides* (*14*). Three polypeptides, the L, H, and M subunits, form this protein complex. They bind nine cofactors: four bacteriochlorophylls, two bacteriopheophytins, two ubiquinones (UQ), and one non-heme iron. The cofactors are arranged in the two branches A and B related by a C_2 symmetry and extend from the special pair to the quinones. Only the A-branch is electron-transfer active. Its cofactors are predominantly embedded in the L subunit. Electronic excitation of the special pair, a bacteriochlorophyll dimer, induces a multistep electron-transfer process from the special pair to the first UQ, called Q_A. From there the electron moves to Q_B, the second UQ. After this initial reaction, a second electron transfer from Q_A to Q_B and two protonations of Q_B follow, resulting in a dihydroquinone Q_BH_2. The dihydroquinone leaves its binding site and is replaced by an oxidized UQ from the quinone pool.

† This work was supported by the Deutsche Forschungsgemeinschaft SFB 498, Project A5. G.M.U. was a fellow of the Boehringer Ingelheim Fonds.

* Corresponding author. E-mail: knapp@chemie.fu-berlin.de. Fax: +49-30-83853464.

‡ Present address: Department of Molecular Biology, The Scripps Research Institute, TPC-15, 10550 N. Torrey Pines Road, La Jolla, CA 92037.

[1] Abbreviations: bRC, bacterial (photosynthetic) reaction center; FTIR, Fourier transform infrared spectroscopy; MC, Monte Carlo; UQ, ubiquinone; Q_A and Q_B, primary and secondary quinone acceptor in the bRC; *Rb. sphaeroides*, *Rhodobacter sphaeroides*; *Rps. viridis*, *Rhodopseudomonas viridis*.

10.1021/bi000413c CCC: $19.00
Published on Web 08/02/2000

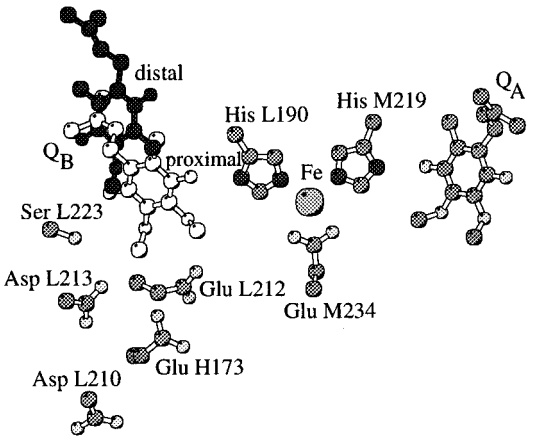

FIGURE 1: Structural arrangement of the quinone binding pockets. View of the two quinones, Q_A and Q_B, the non-heme iron, and selected amino acid side chains from the X-ray structure (*14*). The two different binding sites of Q_B are shown: the distal binding site in the dark-adapted X-ray structure and the proximal binding site in the light-exposed X-ray structure. The exact coordinates of all other atoms shown are taken from the light-exposed X-ray structure, but there are no significant deviations from the coordinates of the dark-adapted X-ray structure. The electron transfer from $Q_A^{\bullet-}$ to Q_B will only occur when Q_B binds at the proximal site. [Drawn with the Molscript program (*73*).]

In previous studies, we investigated several electron-transfer and binding reactions of photosynthetic proteins by various theoretical methods (*15*−*23*). In this work, we focus on the electron transfer from $Q_A^{\bullet-}$ to Q_B in the light-exposed and in the dark-adapted X-ray structures of *Rb. sphaeroides* (*14*). The rate of this electron transfer at low temperatures is dramatically increased in bRC frozen under illumination compared to bRC frozen in the dark (*24*). This effect suggests that the dark-adapted and the light-exposed bRCs differ in their conformation, and the dark-adapted state has to undergo a conformational change before electron transfer can take place efficiently. This conformational change may occur much slower than the electron transfer, which would lead to conformational gating of the reaction (*1*). Conformational gating occurs also in other electron-transfer proteins (*3*) and was proposed for the bRC on the basis of a driving force assay (*2*). Indeed, the X-ray structure (*14*) of the dark-adapted bRC shows that Q_B is displaced by approximately 5 Å and has undergone a 180° propeller twist compared to the structure of the light-exposed bRC (Figure 1). The binding site of Q_B in the dark-adapted bRC is referred to as the distal binding site (with respect to the non-heme iron), whereas the binding site of Q_B in the light-exposed bRC is referred to as the proximal binding site.

In the present study, we calculate the energetics of the electron transfer from $Q_A^{\bullet-}$ to Q_B and the protonation pattern of the titratable groups of the bRC in the dark-adapted and light-exposed X-ray structures by applying a well-established continuum electrostatic method (*25*−*31*). We used this method previously to investigate the coupling of protonation and electron-transfer reactions in the bRC of *Rps. viridis* (*21*, *22*). The main goal of our present work is to investigate the conformational gating hypothesis and to understand how the protein accomplishes the conformational gating.

MATERIALS AND METHODS

Structure. In our calculations, we used the dark-adapted and light-exposed X-ray structures of the bRC from *Rb. sphaeroides* with a resolution of 2.2 and 2.6 Å, respectively (ref *14*; PDB entries 1aij and 1aig, respectively). We considered only the first reaction center in the unit cell (H, L, and M chain together with their cofactors) and ignored the other (N, O, and P chain in 1aig; R, S, and T chain in 1aij). All water and detergent molecules were removed. The influence of water was considered exclusively by a higher dielectric constant in cavities and outside of the protein, because the orientation of the water molecules is not known, which makes their electrostatic effects uncertain (*21*). We used an extended atom representation for the nonpolar hydrogen atoms, except for the quinones, the bacteriochlorophylls, and the bacteriopheophytins, for which all hydrogens were treated explicitly. Polar hydrogens were also treated explicitly, with the exception of the acidic hydrogens of protonated glutamates and aspartates, which were represented by symmetrical charge adjustment of the two carboxyl oxygen atoms as described in ref *21*. Coordinates of explicitly treated hydrogen atoms were generated with Charmm (*32*). The positions of hydrogen atoms were energetically optimized, while the heavy atom positions were fixed. For this optimization, all titratable groups were in their standard protonation (i.e., aspartate, glutamate, the C-termini unprotonated, arginine, cysteine, histidine, lysine, tyrosine, and the N-termini protonated), and both quinones were in their oxidized (uncharged) state. We used the same atomic partial charges as in ref *21*. After the placement of polar hydrogen atoms, Ser-L223 is weakly hydrogen-bonded to Asp-L213, but not to Q_B, in the light-exposed X-ray structure. Ser-L223 does not participate in any hydrogen bond in the dark-adapted X-ray structure.

Calculation of Protonation Patterns. The theoretical background of the calculation of protonation patterns by solving the Poisson−Boltzmann equation and sampling the possible protonation states with a Monte Carlo (MC) method is reviewed in ref *31*. The detailed procedure follows the description in ref *21*. As reported there, we used Bashford's Mead program (*33*, *34*) for the solution of the Poisson−Boltzmann equation. However, for the MC sampling, we used instead of Beroza's Mcti program (*30*) our own program Karlsberg (*35*), which implements the same MC method as Mcti but is equipped with a set of additional features. These features will be reported in detail elsewhere (manuscript submitted). Here, we needed only a subset of them, which comprises triple moves for increased sampling efficiency (*22*), biased MC (*36*), and inclusion of redox groups for the calculation of the redox potentials of the quinones (see next section). The Karlsberg program is freely available under the GNU public license from our webserver (http://lie.chemie.fu-berlin.de/karlsberg/).

All calculations were done for a pH value of 7.0. The dielectric constant in the protein was set to $\epsilon = 4$. A discussion of the choice of this value is given in refs *22*, *29*, and *37*−*39*. For the solvent, we used a dielectric constant of $\epsilon = 80$ and a ionic strength of 100 mM. The Poisson−Boltzmann equation was solved using a three-step grid-focusing procedure with a starting grid resolution of 2.5 Å, an intermediate grid resolution of 1.0 Å, and a final grid resolution of 0.3 Å.

Calculation of the Redox Potential Difference of the Quinones. We treated the quinones as redox-active compounds. The possible protonation of Q_B following the

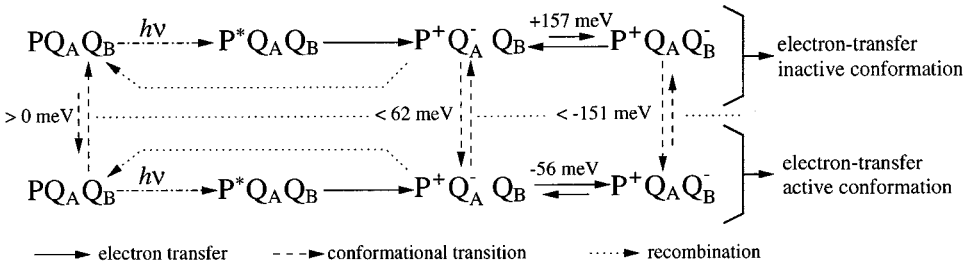

FIGURE 2: Possible electron-transfer reactions and conformational gating in the bRC. The initial reaction is the light excitation of the special pair P to P*, after which a charge separation follows in the sub-microsecond time regime, resulting in the state $P^+Q_A^{\bullet-}Q_B$. The electron is then transferred from $Q_A^{\bullet-}$ to Q_B in the time scale of several hundred microseconds. According to the conformational gating hypothesis, this process involves a conformational transition, after which the actual electron transfer occurs at a much faster rate. Recombination occurs from the state $P^+Q_A^{\bullet-}Q_B$ to PQ_AQ_B with a time constant of about 100 ms. All states can in principle adopt the two conformations considered in the present study: one where the electron transfer from $Q_A^{\bullet-}$ to Q_B is possible and one where it is hindered. We assume that the electron-transfer active conformation is represented by the light-exposed X-ray structure and the electron-transfer inactive conformation by the dark-adapted X-ray structure. The hindering of the electron transfer can be mediated kinetically or thermodynamically (or both). The kinetics is not investigated in the present study, but the thermodynamic result is that the electron transfer is uphill by 157 meV for the dark-adapted X-ray structure, whereas it is downhill by 56 meV for the light-exposed X-ray structure. Due to the experimental conditions, the bRC was in the ground-state PQ_AQ_B for the determination of the dark-adapted X-ray structure and in the charge-separated state $P^+Q_AQ_B^{\bullet-}$ for the determination of the light-exposed X-ray structure. Hence, the conformational equilibrium prefers the electron-transfer inactive conformation in the state PQ_AQ_B and the electron-transfer active conformation in the state $P^+Q_AQ_B^{\bullet-}$. The conformational equilibrium constant in the state $P^+Q_A^{\bullet-}Q_B$ is unknown. The upper limit of 62 meV for the conformational transition in this state is deduced from comparison of experimental and calculated results (see text for details). The upper limit of −151 meV for the conformational transition in the state $P^+Q_AQ_B^{\bullet-}$ results from the thermodynamic cycle connecting the states $P^+Q_A^{\bullet-}Q_B$ and $P^+Q_AQ_B^{\bullet-}$ in the two conformations.

electron transfer (*21*) was not considered here. In principle, a redox-active group can be treated in the same way as a titratable group. The titratable group depends on pH value, which is replaced by the solution redox potential for a redox-active group (*31*, *40*). Here, we consider the two quinones as one extended redox-active group with only two possible redox states: the initial state $Q_A^{\bullet-}Q_B$ and the final state $Q_AQ_B^{\bullet-}$. The transition between these two states does not depend on the solution redox potential and corresponds to an internal electron transfer. This transition was included in the move set of the MC sampling. After MC sampling, we calculated the free energy difference of the two states by using the equation:

$$\Delta G = -k_B T \ln\frac{\langle x\rangle}{1-\langle x\rangle} \qquad (1)$$

where $\langle x\rangle$ and $1-\langle x\rangle$ are the average occupancies of the final and initial state, respectively, k_B is the Boltzmann constant, and T is the absolute temperature. The calculated energy value is derived from electrostatical terms. Thus, it does not include any van der Waals interactions.

If the free energy difference ΔG is not close to zero, the probability $\langle x\rangle$ is close to zero or unity and thus even a small statistical error of the MC sampling leads to a large statistical error of ΔG. To solve this problem, we applied a bias to the sampling of the two redox states (*36*). We chose the bias iteratively such that the probability $\langle x\rangle$ reached a value close to 0.5, which minimized the statistical error of the calculated energy. At the end, the bias was removed from the calculated values to get the original result, but with a strongly reduced statistical error. In two separate MC samplings, we applied also a very large negative or positive bias to obtain protonation patterns with a virtually fixed redox state of the quinones $Q_A^{\bullet-}Q_B$ or $Q_AQ_B^{\bullet-}$, respectively.

RESULTS AND DISCUSSION

Energetics of the Electron Transfer from $Q_A^{\bullet-}$ to Q_B

Review of Experimental Results. The experimental values of the electron-transfer energy are determined by measuring the recombination rates of the bRC states $P^+Q_A^{\bullet-}Q_B$ and $P^+Q_AQ_B^{\bullet-}$ to the ground-state PQ_AQ_B. For the $P^+Q_AQ_B^{\bullet-}$ decay, direct recombination is negligible (*41*−*43*). Instead, it is assumed that the state $P^+Q_AQ_B^{\bullet-}$ is in equilibrium with the state $P^+Q_A^{\bullet-}Q_B$ and recombination occurs nearly exclusively from $P^+Q_A^{\bullet-}Q_B$ (Figure 2). Therefore, if the equilibrium between the states $Q_A^{\bullet-}Q_B$ and $Q_AQ_B^{\bullet-}$ is reached fast compared to the recombination rate from $P^+Q_A^{\bullet-}Q_B$ to the ground state, the equilibrium constant K_{AB} can be calculated from the measured recombination rates with the equation (*44*−*46*):

$$K_{AB} = \frac{k_{AP}}{k_{BP}} - 1 \qquad (2)$$

k_{AP} is the recombination rate from the state $P^+Q_A^{\bullet-}Q_B$, measured in a bRC where electron transfer to Q_B is blocked. k_{BP} is the effective recombination rate from the state $P^+Q_AQ_B^{\bullet-}$. From the equilibrium constant K_{AB}, the reaction energy of the electron transfer from $Q_A^{\bullet-}$ to Q_B can be calculated similarly to eq 1. By this method, the electron-transfer energy was determined by different groups to be −78 meV at pH 7.8 (*47*), −71 meV at pH 8.0 (*44*), nearly constant, −67 meV, from pH 6.0 to pH 8.5 (*45*), or −52 meV at pH 8.1 (*46*).

Computational Results. For the reaction energy of the electron transfer from $Q_A^{\bullet-}$ to Q_B at pH 7, we computed a value of −56 meV for the light-exposed X-ray structure and a value of +157 meV for the dark-adapted X-ray structure (Table 1). According to our computation, the electron transfer

Table 1: Summary of the Computed Results at pH 7.0 for the Dark-Adapted and Light-Exposed X-ray Structure[a]

			protonation probabilities								
	$Q_A^{\bullet-}Q_B \rightarrow Q_AQ_B^{\bullet-}$		$Q_A^{\bullet-}Q_B$			$Q_AQ_B^{\bullet-}$			equilibrium		
structure	energy (meV)	proton uptake	L210	L212	L213	L210	L212	L213	L210	L212	L213
dark (1aij)	+157	0.15 ± 0.03	0.01	0.27	0.75	0.01	0.60	0.85	0.01	0.27	0.75
light (1aig)	−56	0.33 ± 0.02	0.02	0.81	0.37	0.00	1.00	0.99	0.00	0.98	0.93

[a] Shown are the energies for the electron transfer from $Q_A^{\bullet-}$ to Q_B and the protonation probabilities for selected titratable residues in the fixed redox states $Q_A^{\bullet-}Q_B$ and $Q_AQ_B^{\bullet-}$ and in the equilibrium distribution between the two states. L210 and L213 are aspartates, and L212 is a glutamate. The standard deviation of the single-site protonation probabilities is smaller than 0.001 protons.

is energetically uphill in the dark-adapted X-ray structure and downhill in the light-exposed X-ray structure. From a thermodynamic point of view, we can therefore support the assumption that the dark-adapted X-ray structure represents the electron-transfer inactive conformation of the bRC and the light-exposed X-ray structure the electron-transfer active conformation. The implication of this finding for the conformational gating mechanism is discussed in the next section (Conformational Gating). The calculated value for the reaction energy of the electron transfer in the light-exposed X-ray structure is in good agreement with the experimentally determined values. However, this value implies that the bRC adopts completely the electron-transfer active conformation in both states $Q_A^{\bullet-}Q_B$ and $Q_AQ_B^{\bullet-}$, since we have exclusively considered the light-exposed X-ray structure, which is assumed to represent the electron-transfer active conformation. In reality, both states may consist of a mixture of electron-transfer active and inactive conformations as denoted in Figure 2. The possible influence of the distribution of electron-transfer active and inactive conformations on the experimentally determined electron-transfer energy is discussed in the next section (Conformational Gating).

Comparison to Earlier Computations. The energetics of the electron transfer from $Q_A^{\bullet-}$ to Q_B in the bRC from *Rb. sphaeroides* and *Rps. viridis* was investigated several times by electrostatic approaches similar to that used in the present study. The first of these studies was done by Beroza et al. (*36*) on the bRC from *Rb. sphaeroides*. However, they failed to reproduce the experimental value of the electron-transfer energy. The electron transfer was calculated to be uphill by 170 meV. Three years later, we did our own studies on the bRC of *Rps. viridis*, the first without conformational flexibility (*21*), as we did it also in the present study, and the second with conformational relaxation (*22*). In both studies, we could reproduce the experimental value of the electron-transfer energy faithfully. Recently, Alexov and Gunner (*48*) studied the electron transfer from $Q_A^{\bullet-}$ to Q_B also based on the light-exposed and dark-adapted X-ray structures (*14*) as we did it in the present study. Alexov and Gunner took the backbone conformation from the dark-adapted X-ray structure. They generated the side-chain conformers and the binding position of Q_B according to both, the dark-adapted and the light-exposed structures, and several additional bRC structures from *Rb. sphaeroides* and *Rps. viridis*. They included also different conformers of polar hydrogens that are part of a titratable group. The possible combination of conformers were sampled using a generalized MC method (*49*, *50*). In their calculation, explicit water molecules were also included in different orientations, which were also sampled by the MC method. By this method, they included conformational flexibility in their calculations and could reproduce the experimental value for the electron-transfer energy. However, without conformational flexibility, they calculated the electron transfer to be uphill by 165 meV. They reported similar results of R. Lancaster and M. R. Gunner for the bRC from *Rps. viridis* (unpublished results cited in ref *48*).

It is obvious to ask why our own studies reproduce the experimental energy value successfully and all other studies fail. In the past, we proposed as the main reason for our success our detailed charge model for the cofactors of the bRC derived from quantum chemical calculations. In particular, the charges for the non-heme iron center and the quinone in their different redox states (*21*, *22*) differ significantly from those of the simplified charge model used in the other studies (*36*, *48*, *51*). Alexov and Gunner question that assumption and emphasize the fact that the past studies all used different bRC structures (*48*). Without doubt, even moderate conformational changes can have a large effect on electrostatic energies (*22*). R. Lancaster and M. R. Gunner used for their calculation of the electron-transfer energy in the bRC from *Rps. viridis* (unpublished results cited in ref *48*) a new X-ray structure with a better defined Q_B binding site (refs *8* and *9*; PDB code 2prc), which was, however, not publicly available at the time we did our studies. To use the improvements of the new structure anyhow, we applied two well-defined modifications (*21*) to an older X-ray structure (ref *7*; PDB code 1prc) according to information already published at that time (*52*, *53*). By this way, the structure we used for our studies (*21*, *22*) was very similar to that used by R. Lancaster and M. R. Gunner. As soon as the new X-ray structure (*8*, *9*) was publicly available, we repeated our calculation using this structure. Within less than 10 meV, we got the same energy as with our modified structure (unpublished results). Hence, for the bRC from *Rps. viridis*, the structural differences cannot explain the differences in the computational results. However, for the studies on the bRC from *Rb. sphaeroides*, structural differences may be more significant. Beroza et al. (*36*) used another structure (PDB code 4rcr) than Alexov and Gunner (*48*) and us in the present study. Although the latter two studies are based on the same X-ray structures (*14*), the actually used structures differ. We placed polar hydrogens using the Hbuild facility of the program Charmm (*32*) with a subsequent energy minimization (*21*). Alexov and Gunner used the program Proteus (*54*) to place polar hydrogens. We used the original light-exposed and dark-adapted X-ray structure, whereas Alexov and Gunner used for their calculation with a single protein conformation the backbone from the dark structure, which is, however, nearly identical to the backbone of the light structure. They selected for each side chain and for Q_B the conformer with the highest population in their calcula-

tions with conformational flexibility for the ground state of the quinones (Q_AQ_B). This selection procedure leads to a structure that will be energetically optimized for uncharged quinones and may prefer one of the two states $Q_A^{\bullet-}Q_B$ and $Q_AQ_B^{\bullet-}$ more than the other.

To probe our assumption that the different charge models are the most important reason for the different results, we repeated our calculation using the charge model of Alexov and Gunner (*48*, *51*) for the quinones, resulting in an electron-transfer energy of −6 meV, thus an increase of the electron-transfer energy by 50 meV. This is a significant shift but can only partially explain the difference between the calculated energy in this study and the energy calculated for the rigid case in ref *48*. However, the charges of the polypeptides are also different in all three studies and may cause additional significant differences in the electrostatic energy. We used the charges from the Charmm parameter set provided by Molecular Simulations Inc., which closely resemble those of the Charmm 19 parameter set (*32*) but are also available for several amino acids in nonstandard protonation. Alexov and Gunner (*48*, *51*) used Parse charges (*55*), which tend to be more localized and to have larger absolute values than the Charmm charges we used. Beroza et al. (*36*) used charges from the Discover force field (*56*).

In addition to different charge models and different structures, there are a number of other possible differences in the conditions and techniques of solving the Poisson−Boltzmann equation. Most evident is the resolution of the employed grid. We used a grid with a lattice constant of 0.3 Å, whereas Alexov and Gunner used a relatively coarse grid with a lattice constant of 0.83 Å. Also, the inclusion of explicit water molecules can have a significant effect. Alexov and Gunner included explicit water molecules in their calculation with conformational flexibility. This is reasonable since the water molecules can adopt different orientations in such a calculation. In a calculation with a rigid conformation, the inclusion of explicit water molecules is dangerous if the correct orientation is unknown. However, it is not clear whether Alexov and Gunner included explicit water molecules in their calculation for the rigid protein. In ref *48*, there are contradicting statements in connection with Figure 9 that "waters were deleted" and "waters are rigid".

Conformational Gating

Review of Experimental Results. Conformational gating (*1*) was proposed for the bRC of *Rb. sphaeroides* on the basis of experiments in which the driving force for the electron transfer from $Q_A^{\bullet-}$ to Q_B was varied (*2*). In this experiment, Q_A was replaced by quinones other than UQ that have different redox potentials. The electron-transfer rate from $Q_A^{\bullet-}$ to Q_B was not changed significantly by this replacement. The reaction energy of the electron transfer is relatively small so that the electron-transfer process occurs in the normal regime, where the classical Marcus theory (*4*, *5*) predicts a strong dependency of the electron-transfer rate on the reaction energy. The observed independency of the electron-transfer rate on the reaction energy can be explained by a conformational gating mechanism. According to the conformational gating mechanism, the bRC can adopt two conformations: an electron-transfer active conformation and an electron-transfer inactive conformation (Figure 2). The electron transfer from $Q_A^{\bullet-}$ to Q_B will occur nearly exclusively in the electron-transfer active conformation. In the ground-state PQ_AQ_B, the bRC is preferentially in the electron-transfer inactive conformation. Hence, a conformational transition is necessary to allow the electron transfer from $Q_A^{\bullet-}$ to Q_B. This transition is the rate-determining step.

To determine the two conformations experimentally, X-ray structures were solved of the dark-adapted bRC, which is in the ground-state PQ_AQ_B, and of the light-exposed bRC, which was frozen immediately after illumination and therefore in the state $P^+Q_AQ_B^{\bullet-}$ (*14*). The most striking difference between the two X-ray structures is the displacement of Q_B from a binding site proximal to the non-heme iron to a distal binding site. In the light-exposed X-ray structure, Q_B binds at the proximal binding site, whereas in the dark-adapted X-ray structure it binds at the distal binding site (Figure 1). However, the electron density at the proximal binding site suggests a partial occupancy of Q_B at the proximal site even in the dark-adapted X-ray structure. It was proposed that the dark-adapted and light-exposed X-ray structures represent the electron-transfer inactive and active conformations, respectively. Thus, in the state $P^+Q_AQ_B^{\bullet-}$ the equilibrium between electron-transfer inactive and active conformations prefers the electron-transfer active conformation, and in the ground-state PQ_AQ_B it prefers the electron-transfer inactive conformation. The detected partial occupancy of Q_B at the proximal binding site shows that the preference of the equilibrium for the electron-transfer inactive or active conformation is less pronounced in the ground state than in the state $P^+Q_AQ_B^{\bullet-}$ (Figure 2).

This finding is in agreement with kinetic measurements that found the electron-transfer rate from $Q_A^{\bullet-}$ to Q_B to be at least biphasic (*57*, *58*). The fast phase can be assigned to the electron transfer in the electron-transfer active conformation and the slow phase to the conformational transition from the electron-transfer inactive conformation to the electron-transfer active conformation. However, the quantitative results of the two kinetic studies (*57*, *58*) are very different and seem to be highly sensitive to the details of the experimental procedure. The fast rate component of the total reaction yield, which is according to our interpretation identical to the occupancy of the electron-transfer active conformation in the ground state, was measured to be 25% by Tiede et al. (*57*) and 60% by Li et al. (*58*). A strong preparation dependency was explicitly reported and discussed (*57*). The reported distributions are, however, not very different in terms of free energy. This means that very subtle changes of conditions may have a strong influence on the observed distribution for both experiment and calculation. We conclude, that the free energy difference between electron-transfer active and inactive conformations is close to zero and its exact value depends on the experimental conditions.

Computational Results. As mentioned above, we computed the reaction energy of the electron transfer from $Q_A^{\bullet-}$ to Q_B to be uphill by 157 meV in the dark-adapted X-ray structure. We can therefore support the assumption that the dark-adapted X-ray structure is electron-transfer inactive. Our viewpoint is exclusively thermodynamic. There may also be kinetic reasons for the inhibition of the electron transfer in the dark-adapted X-ray structure (*14*), but we did not consider

kinetics in the present study. In the following, we assume that the amount of electron transfer between Q_A and Q_B in the dark-adapted X-ray structure is negligibly small.

From the results above, we concluded that the equilibrium between electron-transfer active and inactive conformations prefers strongly the active conformation in the state $P^+Q_AQ_B^{\bullet-}$ and only weakly the inactive conformation in the ground-state PQ_AQ_B (Figure 2). The value of the conformational equilibrium constant in the state $P^+Q_A^{\bullet-}Q_B$ is unknown, but it would have implications for the detailed mechanism of the conformational gating. Depending on the value of the equilibrium constant, the gating mechanism is between the following two limiting cases:

(i) The equilibrium constant could be the same in the states PQ_AQ_B and $P^+Q_A^{\bullet-}Q_B$. Electron transfer from $Q_A^{\bullet-}$ to Q_B will only occur in the small fraction of bRCs in the electron-transfer active conformation. After electron transfer, the equilibrium between electron-transfer active and inactive conformations readjusts by a conformational transition, and further electron transfer occurs with the effective rate of the conformational transition. In this mechanism, the Q_B reduction "pulls" the bRC into the electron-transfer active conformation. Hence, we call this mechanism a *pull transition*.

(ii) The equilibrium constant could be the same in the states $P^+Q_A^{\bullet-}Q_B$ and $P^+Q_AQ_B^{\bullet-}$; i.e., already the reduction of Q_A (or other light-induced events going along with the Q_A reduction) triggers the transition to the electron-transfer active conformation (*2*). In this case, the conformational transition from the inactive to the active conformation would also occur without the electron transfer from $Q_A^{\bullet-}$ to Q_B. The bRC is "pushed" into the electron-transfer active conformation, whether the electron transfer from $Q_A^{\bullet-}$ to Q_B will actually occur or not. We call this mechanism a *push transition*. Since the electron-transfer reaction that leads from the state $P^*Q_AQ_B$ to the state $P^+Q_A^{\bullet-}Q_B$ is in the sub-millisecond time regime, the much slower conformational transition is still the rate-limiting step and the electron-transfer reaction is therefore still gated. This rate limitation can only be circumvented by fixing the bRC in the state $P^+Q_A^{\bullet-}Q_B$, waiting until the conformational transition to the electron-transfer active conformation has occurred, and then releasing the fixation, so that the electron transfer can proceed ungated. This procedure is, however, only a *Gedankenexperiment* and could probably not be done in reality.

The equilibrium constant between the electron-transfer active and inactive conformations in the state $P^+Q_A^{\bullet-}Q_B$ can be calculated from the difference between the calculated and experimentally measured reaction energies of the electron transfer from $Q_A^{\bullet-}$ to Q_B as shown in the following: We neglect, as mentioned above, the electron transfer between Q_A and Q_B in the electron-transfer inactive conformation. We also neglect the occupancy of the state $P^+Q_AQ_B^{\bullet-}$ in the electron-transfer inactive conformation compared to the occupancy of the same state in the electron-transfer active conformation. With these assumptions, two equilibria remain: one is the equilibrium between $P^+Q_A^{\bullet-}Q_B$ and $P^+Q_AQ_B^{\bullet-}$ in the electron-transfer active conformation with the corresponding equilibrium constant K_{AB}, and the other is the equilibrium between the electron-transfer active (act) and inactive (inact) conformations of the state $P^+Q_A^{\bullet-}Q_B$ with the corresponding equilibrium constant K_{conf} (Figure 2):

$$K_{AB} = \frac{[P^+Q_AQ_B^{\bullet-}\text{act}]}{[P^+Q_A^{\bullet-}Q_{B\,act}]} = \exp\left(-\frac{\Delta G_{AB}}{kT}\right) \quad (3)$$

$$K_{conf} = \frac{[P^+Q_A^{\bullet-}Q_{B\,act}]}{[P^+Q_A^{\bullet-}Q_{B\,inact}]} = \exp\left(-\frac{\Delta G_{conf}}{kT}\right) \quad (4)$$

Both equilibria are reached fast compared to the recombination rate from $P^+Q_A^{\bullet-}Q_B$ to the ground state (*46*). In our calculation, we evaluated the equilibrium constant K_{AB}, whereas the above-described experimental method to measure the equilibrium of the states $P^+Q_A^{\bullet-}Q_B$ and $P^+Q_AQ_B^{\bullet-}$ yields an equilibrium constant K_{exp} that describes the equilibrium of the states $P^+Q_A^{\bullet-}Q_B$ and $P^+Q_AQ_B^{\bullet-}$ in both conformations, the electron-transfer active and inactive. Since the occupancy of the state $P^+Q_AQ_B^{\bullet-}$ in the electron-transfer inactive conformation is neglected here, the expression of the experimentally determined equilibrium constant simplifies to

$$K_{exp} = \frac{[P^+Q_AQ_B^{\bullet-}\text{act}]}{[P^+Q_A^{\bullet-}Q_{B\,act}] + [P^+Q_A^{\bullet-}Q_{B\,inact}]} = \exp\left(-\frac{\Delta G_{exp}}{kT}\right) \quad (5)$$

The connection between the three equilibrium constants is

$$K_{conf} = \frac{K_{exp}}{K_{AB} - K_{exp}} \quad (6)$$

Using eq 1, the equilibrium constants in eq 6 can be converted into free energy, yielding the following expression for the free energy of the conformational transition in the state $P^+Q_A^{\bullet-}Q_B$:

$$\Delta G_{conf} = kT \ln\left[\exp\left(\frac{\Delta G_{exp} - \Delta G_{AB}}{kT}\right) - 1\right] \quad (7)$$

ΔG_{exp} is the experimentally determined reaction energy of the electron transfer from $Q_A^{\bullet-}$ to Q_B derived from K_{exp}, and ΔG_{AB} is the calculated reaction energy of the electron transfer from $Q_A^{\bullet-}$ to Q_B for the fixed electron-transfer active conformation derived from K_{AB}.

Since the differences between ΔG_{exp} and ΔG_{AB} are within experimental and computational uncertainty, ΔG_{conf} can only be estimated roughly. The experimental values for ΔG_{exp} range from -78 to -52 meV (*44*−*47*). The uncertainty of our computational result is very difficult to estimate because the intrinsic error of our electrostatic model is unknown. However, we assume, on the basis of our and others experiences, that our electrostatic model is sufficiently accurate to be applied successfully. We would call an electrostatic calculation of reaction energy successful if it reproduces experimental result with an error of about ± 60 meV, which is equivalent to ± 1 p*K* unit. We assume this value to be the uncertainty of our computational result due to the potential error of the underlying model (but not due to errors in the computation itself). Hence, the value for the

difference $\Delta G_{exp} - \Delta G_{AB}$ is in the range from −82 to +64 meV. A negative value of this difference is not possible, so that the remaining range is from 0 to +64 meV. A value of 0 meV corresponds to an infinitely negative value for ΔG_{conf}, which means that the electron-transfer inactive conformation is unpopulated in the state $P^+Q_A^{\bullet-}Q_B$ (when equilibrium is reached) and the conformational gating is done by a push transition as described above. A value of +64 meV for the difference $\Delta G_{exp} - \Delta G_{AB}$ corresponds to a value for ΔG_{conf} of +62 meV or an equilibrium distribution of about 90% electron-transfer inactive conformation and 10% electron-transfer active conformation in the state $P^+Q_A^{\bullet-}Q_B$. Such a distribution is, at least in terms of free energy, very similar to those observed by the kinetic experiments for the ground state (*57*, *58*). This means that the distribution of the electron-transfer active and inactive conformations is similar in the ground-state PQ_AQ_B and in the state $P^+Q_A^{\bullet-}Q_B$, so that the conformational gating is done by a pull transition.

We conclude that the free energy of the transition between electron-transfer active and inactive conformations in the state $P^+Q_A^{\bullet-}Q_B$ is smaller than 62 meV. Following the thermodynamic cycle in the right part of Figure 2, we can calculate the free energy of the transition between electron-transfer active and inactive conformations in the state $P^+Q_AQ_B^{\bullet-}$ to be smaller than −151 meV, which is in agreement with previous conclusions. However, from our results we cannot decide whether the conformational gating is mediated preferentially via a push transition or a pull transition.

Comparison to Earlier Computations. In the already discussed study of Alexov and Gunner (*48*) the dark-adapted and light-exposed X-ray structures were not considered separately, but in one calculation where the different side chain, Q_B, and water conformers were sampled together with the titration states by a generalized MC method. They included the two binding modes of the Q_B, distal and proximal, in the sampling. For the state $P^+Q_AQ_B^{\bullet-}$, Q_B was completely localized at the proximal binding site, and the distal binding side was not populated in agreement with the light-exposed X-ray structure (*14*). For the ground-state PQ_AQ_B and the state $P^+Q_A^{\bullet-}Q_B$, the distal binding site was occupied to 20% and the proximal binding site to 80%. This is in contradiction with the dark-adapted X-ray structure, which suggests that in the ground state the preferred binding site of Q_B is the distal site (*14*). However, as discussed above, the conformational transition from the electron-transfer inactive to the active conformation, which means mostly the movement of Q_B from the distal to the proximal binding site, is energetically very easy and may even be triggered by certain experimental conditions. The movement of Q_B was recently observed in a molecular dynamics simulation (*59*), where it was triggered by a change of the protonation pattern of the residues Glu-L212 and Asp-L213 (see next section). So the contradiction of the computational results of Alexov and Gunner and the X-ray structure does not necessarily mean that there is a severe problem with the computational model. In agreement with our results, the electron transfer to Q_B bound at the distal site was reported to be unfavorable, but a value of the reaction energy was not provided. Alexov and Gunner proposed that possibly several smaller conformational changes and not the transition of Q_B from the distal to the proximal binding site is most important for the conformational gating process. They concluded this from their finding that the electron transfer from $Q_A^{\bullet-}$ to Q_B is uphill if they do not include conformational relaxation in their calculation (see above). However, in our studies without conformational flexibility for *Rb. sphaeroides* (this study) and *Rps. viridis* (*21*), we obtained energy values for the electron transfer from $Q_A^{\bullet-}$ to Q_B that are in good agreement with experimental values. The introduction of conformational relaxation for the bRC from *Rps. viridis* did not change our results fundamentally (*22*).

Protonation Patterns of the Titratable Groups

Review of Experimental Results. According to some experiments measuring directly the proton uptake (*60*, *61*), the proton uptake of the whole bRC due to the electron transfer from $Q_A^{\bullet-}$ to Q_B at pH 7.0 is close to zero. Also, the pH independence of the electron-transfer energy in the pH range between 6 and 8.5 (*45*) implies no proton uptake. Other measurements of proton uptake, however, suggest an uptake of about 0.5 proton (*62*, *63*) upon electron transfer from Q_A to Q_B. The direct measurement of proton uptake is supposed to be less reliable than the measurement of the pH dependency of the electron-transfer energy.

Also, the protonation behavior of individual titratable groups is controversial. On one hand, there are several FTIR studies (*64*−*68*) that suggest that no significant proton uptake of carboxylic groups occurs upon $Q_B^{\bullet-}$ formation in the bRC from *Rb. sphaeroides* (*64*−*66*) as well as from *Rps. viridis* (*67*, *68*), with the only exception of Glu-L212 in the bRC from *Rb. sphaeroides*, which takes up 0.3−0.4 proton (*64*, *65*). Especially, Glu-H173 and Asp-L213 were reported not to contribute significantly to proton uptake (*66*). On the other hand, there are other studies on wild-type and mutant bRCs from *Rb. sphaeroides*, investigating electron-transfer rates (*69*) and the pH-dependent proton uptake (*70*, *71*) and electrogenic events (*61*) upon $Q_B^{\bullet-}$ formation. The measurements of pH-dependent proton uptake (*70*, *71*) and electrogenic events (*61*) assign a p*K* value of about 9.5 to Glu-L212, resulting in an essentially protonated Glu-L212 at neutral pH, which does not change its protonation state. The discrepancy between these results and the FTIR studies may be resolved by assuming a nonclassical titration behavior of Glu-L212 (*61*). This assumption is reasonable, because Glu-L212 is part of a strongly coupled cluster of titratable groups. However, the study of Paddock et al. (*69*) suggests that also at pH 7.5 Glu-L212 is always protonated and Asp-L213 is a more probable candidate for proton uptake. The reason for this contradiction may be the uncertainties in interpreting experimental results. Especially the common assignment of measured results to certain residues by mutation studies may be wrong if the mutation causes unexpected conformational and electrostatic effects in the bRC. For the FTIR studies, another explanation was suggested on the basis of observed IR signatures for highly polarizable hydrogen bond networks, suggesting that the protons taken up upon quinone reduction tend to reside more on the bound water molecules of the network than on carboxylic groups themselves, which would make them invisible for FTIR measurements (*68*, *72*).

Computational Results. According to our computations, the bRC from *Rb. sphaeroides* takes up 0.33 proton in the

light-exposed X-ray structure and 0.15 proton in the dark-adapted X-ray structure upon electron transfer from $Q_A^{\bullet-}$ to Q_B. The total proton uptake of the dark-adapted X-ray structure is not relevant, because electron transfer will not occur in this structure. The total proton uptake of the light-exposed X-ray structure is in reasonable agreement with the experiments that suggest such a proton uptake (*62*, *63*) but does not support the experiments that did not find any proton uptake (*60*, *61*). The proton uptake of the bRC due to the electron transfer from $Q_A^{\bullet-}$ to Q_B is determined experimentally by comparing the proton uptake of the native bRC and of a bRC where electron transfer from $Q_A^{\bullet-}$ to Q_B is blocked. In both cases, the bRCs are excited by a single flash from the ground state to the state $P^+Q_AQ_B^{\bullet-}$ and $P^+Q_A^{\bullet-}Q_B$, respectively. The blocking is usually accomplished by replacing Q_B by a redox-inactive compound like terbutryn. This replacement may, however, significantly change the protonation behavior of the bRC upon reduction of Q_A, since the Q_A reduction also affects the environment of Q_B (*62*). In addition, the transition from the electron-transfer inactive to the active conformation consists mainly of the movement of Q_B from the distal to the proximal binding site. Since Q_B is exchanged by a different compound, the characteristics of the conformational transition, which is anyway strongly dependent on the experimental conditions, will be modified. Our results show a significantly different protonation behavior for the dark-adapted and light-exposed X-ray structures (see also below). Hence, an explanation for the different experimental results may be a modification of the conformational transition and thus of the protonation behavior, depending on the compound used for blocking the electron transfer and other experimental details.

In Table 1, the protonation probabilities of the aspartates L210 and L213 and of the glutamate L212 are shown. These three residues constitute a strongly coupled cluster of titratable groups in close proximity to Q_B. They are the only groups with nonstandard protonation probability within a distance of 10 Å from Q_B (see also Figure 1). The protonation pattern of such a coupled cluster can be altered dramatically by small energy changes if the p*K* values of the individual titratable groups are not too different and no net protonation or deprotonation of the whole cluster occurs. This effect has to be kept in mind for the following discussion of the detailed distribution of protons within the cluster. The equilibrium between the redox states $Q_A^{\bullet-}Q_B$ and $Q_AQ_B^{\bullet-}$ is for the dark-adapted X-ray structure strongly inclined to the state $Q_A^{\bullet-}Q_B$ and for the light-exposed X-ray structure to the state $Q_AQ_B^{\bullet-}$. Hence, the entries in the column "equilibrium" of Table 1 are similar to those of the $Q_A^{\bullet-}Q_B$ state for the dark-adapted X-ray structure and similar to those of the $Q_AQ_B^{\bullet-}$ state for the light-exposed X-ray structure. When the electron-transfer reaction between $Q_A^{\bullet-}$ and Q_B is equilibrated, the cluster of the three strongly coupled residues Asp-L210, Glu-L212, and Asp-L213 contains two protons in the light structure but only one proton in the dark structure. The proton uptake of the coupled cluster is for both the light-exposed and dark-adapted X-ray structures more than twice as large as the total proton uptake of the whole bRC. Hence, more than half of the proton uptake of the cluster is compensated by numerous small protonation changes in the network of titratable groups farther away from Q_B. The only large protonation changes occur at Glu-L212 and Asp-L213. With the exception of Asp-L213, this is in agreement with the FTIR results (*64*−*66*). If the protonation of Glu-L212 and Asp-L213 is compared in the states $Q_A^{\bullet-}Q_B$ and $Q_AQ_B^{\bullet-}$ for the light-exposed X-ray structure, Asp-L213 takes up 0.5 proton and Glu-L212 is mostly protonated in both states with a takeup of only 0.2 proton. These results are in agreement with the non-FTIR results (*61*, *69*−*71*). However, if the state $Q_A^{\bullet-}Q_B$ for the dark-adapted X-ray structure is compared with the state $Q_AQ_B^{\bullet-}$ for the light-exposed X-ray structure, which means that the conformational transition is included in the comparison, Glu-L212 takes up 0.7 proton and now Asp-L213 is mostly protonated in both states with a takeup of only 0.2 proton. These results are more in agreement with the FTIR results (*64*−*66*). Besides the already discussed possible reasons for the described contradictions (see section Review of Experimental Results above), now another explanation comes into mind. It seems to be critical for the experimental result whether under certain experimental conditions the measurement includes or excludes the conformational transition. So it may be rewarding to further investigate the events that trigger the conformational transition (*2*).

Comparison to Earlier Computations. In a recent molecular dynamics study also based on the dark-adapted and light-exposed X-ray structures (*14*), Grafton and Wheeler investigated the protonation states of Glu-L212 and Asp-L213 (*59*). They found in agreement with our own results that $Q_B^{\bullet-}$ binding at the proximal binding site is only possible when both residues are protonated, whereas binding of the neutral Q_B at the distal site is most consistent with one residue protonated and the other unprotonated. In agreement with non-FTIR experimental results (*69*), they propose that the proton binds preferentially at Glu-L212 and not at Asp-L213.

The most significant difference in protonation patterns between this study and that of Alexov and Gunner already discussed above (*48*) is the protonation of Glu-L212 and Asp-L210. While we calculated a protonation change of Glu-L212 of 0.2−0.7 (depending on including the conformational transition or not) in reasonable agreement with FTIR results (*64*−*66*), in ref *48* Glu-L212 was found to be always protonated. According to ref *48*, a large protonation change is localized at Asp-L210, which is always nearly unprotonated in our study.

Two studies on the bRC of *Rps. viridis* applied similar methods as the present one. The first was done by Lancaster et al. (*51*), and the second is our own study (*21*). FTIR difference spectra for Q_B minus $Q_B^{\bullet-}$ show large differences between the bRCs from *Rb. sphaeroides* and *Rps. viridis* (*66*). According to the FTIR results (*67*, *68*), the protonation of Glu-L212 on the bRC of *Rps. viridis* does not change upon $Q_B^{\bullet-}$ formation. Asp-L213 is replaced by the nontitratable, neutral residue Asn. So it is interesting to investigate the differences in the protonation pattern between the bRCs from *Rb. sphaeroides* and *Rps. viridis*. The study of Lancaster et al. (*51*) shows protonation changes localized at the residues Glu-H177, Glu-L212, and Glu-M234. The protonation change of carboxylic groups is in contradiction with the FTIR experiments that suggest no proton uptake of carboxylic groups at all (*67*, *68*). However, the reported

protonation changes are all small (0.15 proton per titratable group or less). In our own study (*21*), Glu-L212 is in agreement with the experiments always protonated. The change of protonation is mainly localized at Glu-H177, which corresponds to Glu-H173 in the bRC of *Rb. sphaeroides*. Glu-H177 takes up 0.5 proton upon $Q_B^{\bullet-}$ formation, which does not agree with the FTIR results (*67*, *68*). However, also in this case it might be possible that, for a highly polarizable hydrogen bond network involving Glu-L212 and Glu-H177, protons reside in part also at bound water molecules, which could make them invisible for FTIR measurements concentrating on the carboxylic groups (*68*, *72*).

CONCLUSION

We calculated the energy of the electron-transfer process from $Q_A^{\bullet-}$ to Q_B in the bRC from *Rb. sphaeroides* for the light-exposed and dark-adapted X-ray structures. For the light-exposed X-ray structure, we got an energy value of −56 meV, which is in agreement with experimental values. For the dark-adapted X-ray structure, the electron transfer was calculated to be uphill by 157 meV. Thus, from a thermodynamic point of view, we can support the assumption that the dark-adapted X-ray structure represents the electron-transfer inactive conformation and the light-exposed X-ray structure the electron-transfer active conformation of a conformational gating model. The main difference between the two X-ray structures is the binding position of Q_B (Figure 1). We disagree with the assumption that numerous conformational changes independent from the Q_B binding position and not represented in the X-ray structures are necessary for the electron transfer and responsible for the conformational gating mechanism, because we did not need to consider such conformational variability in our calculation to get agreement with experimental values. There are numerous differences between our present and recent studies on one hand and other theoretical studies on the other hand, which may explain why the other studies failed to reproduce experimental values without considering conformational flexibility explicitly. The most important differences are a cruder charge model for the cofactors, a different charge model for the polypeptides, a larger grid spacing in the electrostatic calculation, and the use of a different structure.

We also calculated protonation patterns for the $Q_A^{\bullet-}Q_B$ and the $Q_AQ_B^{\bullet-}$ states, which in most details agree with experiments. Our results suggest that triggering of the transition from the electron-transfer inactive to the electron-transfer active conformation of the bRC will significantly change the protonation behavior of the whole bRC and of individual titratable groups. The question of whether this triggering takes place during a measurement under certain experimental conditions was not considered for the interpretation of experimental results so far. A careful investigation of the triggering of the conformational change may resolve some of the contradictions between experimental results for the same quantities determined by different methods or under different experimental conditions.

ACKNOWLEDGMENT

We thank Dr. Donald Bashford and Dr. Martin Karplus for providing the programs Mead and Charmm, respectively.

REFERENCES

1. Davidson, V. C. (1996) *Biochemistry 35*, 14035−14039.
2. Graige, M. S., Feher, G., and Okamura, M. Y. (1998) *Proc. Natl. Acad. Sci. U.S.A. 95*, 11679−11684.
3. Zhou, J. S., and Kostić, N. M. (1993) *J. Am. Chem. Soc. 115*, 10796−10804.
4. Marcus, R. A. (1956) *J. Chem. Phys. 24*, 966−978.
5. Marcus, R. A., and Sutin, N. (1985) *Biochim. Biophys. Acta 811*, 265−322.
6. Deisenhofer, J., Epp, O., Miki, K., Huber, R., and Michel, H. (1985) *Nature 318*, 618−624.
7. Deisenhofer, J., Epp, O., Sinning, I., and Michel, H. (1995) *J. Mol. Biol. 246*, 429−457.
8. Lancaster, C. R. D., and Michel, H. (1997) *Structure 5*, 1339−1359.
9. Lancaster, C. R. D., and Michel, H. (1999) *J. Mol. Biol. 286*, 883−898.
10. Allen, J. P., Feher, G., Yeates, T. O., Komiya, H., and Rees, D. C. (1987) *Proc. Natl. Acad. Sci. U.S.A. 84*, 6162−6166.
11. Chang, C. H., El-Kabbani, O., Riede, D., Norris, J., and Schiffer, M. (1991) *Biochemistry 30*, 5353−5360.
12. Ermler, U., Fritzsch, G., Buchanan, S. K., and Michel, H. (1994) *Structure 2*, 925−936.
13. Arnoux, B., Gaucher, J.-F., Ducruix, A., and Reiss-Husson, F. (1995) *Acta Crystallogr. D 51*, 368−379.
14. Stowell, M. H. B., McPhillips, T. M., Rees, D. C., Soltis, S. M., Abresch, E., and Feher, E. (1997) *Science 276*, 812−816.
15. Muegge, I., Ermler, U., Fritsch, G., and Knapp, E. W. (1995) *J. Phys. Chem. 99*, 89−100.
16. Ullmann, G. M., and Kostić, N. M. (1995) *J. Am. Chem. Soc. 117*, 4766−4774.
17. Muegge, I., Apostolakis, J., Ermler, U., Fritzsch, G., Lubitz, W., and Knapp, E. W. (1996) *Biochemistry 35*, 8359−8370.
18. Apostolakis, J., Muegge, I., Ermler, U., Fritzsch, G., and Knapp, E. W. (1996) *J. Am. Chem. Soc. 118*, 3743−3752.
19. Ullmann, G. M., Hauswald, M., Jensen, A., Kostić, N. M., and Knapp, E. W. (1997) *Biochemistry 36*, 16187−16196.
20. Ullmann, G. M., Knapp, E. W., and Kostić, N. M. (1997) *J. Am. Chem. Soc. 119*, 42−52.
21. Rabenstein, B., Ullmann, G. M., and Knapp, E. W. (1998) *Biochemistry 37*, 2488−2495.
22. Rabenstein, B., Ullmann, G. M., and Knapp, E. W. (1998) *Eur. Biophys. J. 27*, 626−637.
23. Ullmann, G. M., Hauswald, M., Jensen, A., and Knapp, E. W. (2000) *Proteins 38*, 301−309.
24. Kleinfeld, D., Okamura, M. Y., and Feher, G. (1984) *Biochemistry 23*, 5780−5786.
25. Gilson, M. K., and Honig, B. H. (1986) *Biopolymers 25*, 2097−2119.
26. Nicholls, A., and Honig, B. (1991) *J. Comput. Chem. 12*, 435−445.
27. Davis, M. E., and McCammon, J. A. (1991) *J. Comput. Chem. 12*, 909−912.
28. Bashford, D., and Karplus, M. (1991) *J. Phys. Chem. 95*, 9557−9561.
29. Honig, B., and Nicholls, A. (1995) *Science 268*, 1144−1149.
30. Beroza, P., Fredkin, D. R., Okamura, M. Y., and Feher, G. (1991) *Proc. Natl. Acad. Sci. U.S.A. 88*, 5804−5808.
31. Ullmann, G. M., and Knapp, E. W. (1999) *Eur. Biophys. J. 28*, 533−551.
32. Brooks, B. R., Bruccoleri, R. E., Olafson, B. D., States, D. J., Swaminathan, S., and Karplus, M. (1983) *J. Comput. Chem. 4*, 187−217.
33. Bashford, D., and Gerwert, K. (1992) *J. Mol. Biol. 224*, 473−486.
34. Bashford, D. (1997) in *Scientific Computing in Object-Oriented Parallel Environments* (Ishikawa, Y., Oldehoeft, R. R., Reynders, J. V. W., and Tholburn, M., Eds.) Lecture Notes in Computer Science, Vol. 1343, pp 233−240, Springer, Berlin.
35. Rabenstein, B. (1999) *Karlsberg online manual* (http://lie.chemie.fu-berlin/karlsberg/).
36. Beroza, P., Fredkin, D. R., Okamura, M. Y., and Feher, G. (1995) *Biophys. J. 68*, 2233−2250.

37. Warshel, A., and Russel, S. T. (1984) *Q. Rev. Biophys. 17*, 283−422.
38. Warshel, A., and Åqvist, J. (1991) *Annu. Rev. Biophys. Biophys. Chem. 20*, 267−298.
39. Warshel, A., Papazyan, A., and Muegge, I. (1997) *J. Biol. Inorg. Chem. 2*, 143−152.
40. Ullmann, G. M. (2000) *J. Phys. Chem. B 104*, 6293−6301.
41. Kleinfeld, D., Okamura, M. Y., and Feher, G. (1982) *Biophys. J. 37*, 110a.
42. Wraight, C. A. (1979) *Biochim. Biophys. Acta 548*, 309−327.
43. Wraight, C. A., and Stein, R. R. (1980) *FEBS Lett. 113*, 73−77.
44. Mancino, L. J., Dean, D. P., and Blankenship, R. E. (1984) *Biochim. Biophys. Acta 764*, 46−54.
45. Kleinfeld, D., Okamura, M. Y., and Feher, G. (1984) *Biochim. Biophys. Acta 766*, 126−140.
46. Tandori, J., Sebban, P., Michel, H., and Baciou, L. (1999) *Biochemistry 38*, 13179−13187.
47. Arata, H., and Parson, W. W. (1981) *Biochim. Biophys. Acta 638*, 201−209.
48. Alexov, E. G., and Gunner, M. R. (1999) *Biochemistry 38*, 8253−8270.
49. Beroza, P., and Case, D. A. (1996) *J. Phys. Chem. 100*, 20156−20163.
50. Alexov, E. G., and Gunner, M. R. (1997) *Biophys. J. 74*, 2075−2093.
51. Lancaster, C. R. D., Michel, H., Honig, B., and Gunner, M. R. (1996) *Biophys. J. 70*, 2469−2492.
52. Lancaster, C. R. D., and Michel, H. (1996) in *The Reaction Center of Photosynthetic Bacteria* (Michel-Beyerle, M.-E., Ed.) pp 23−35, Springer, Berlin.
53. Lancaster, C. R. D., Ermler, U., and Michel, H. (1995) in *Anoxygenic Photosynthetic Bacteria* (Blankenship, R. E., Madigan, M. T., and Bauer, C. E., Eds.) pp 503−526, Kluwer Academic Publishers, Dordrecht.
54. Gunner, M. R., Nicholls, A., and Honig, B. (1996) *J. Phys. Chem. 100*, 4277−4291.
55. Sitkoff, D., Sharp, K. A., and Honig, B. (1994) *J. Phys. Chem. 98*, 1978−1988.
56. Hagler, A. T., Huler, E., and Lifson, S. (1974) *J. Am. Chem. Soc. 96*, 5319−5335.
57. Tiede, D. M., Vázquez, J., Córdova, J., and Marone, P. A. (1996) *Biochemistry 35*, 10763−10775.
58. Li, J., Gilroy, D., Tiede, D. M., and Gunner, M. R. (1998) *Biochemistry 37*, 2818−2829.
59. Grafton, A. K., and Wheeler, R. A. (1999) *J. Phys. Chem. B 103*, 5380−5387.
60. McPherson, P. H., Okamura, M. Y., and Feher, G. (1988) *Biochim. Biophys. Acta 934*, 348−368.
61. Brzezinski, P., Paddock, M. L., Okamura, M. Y., and Feher, G. (1997) *Biochim. Biophys. Acta 1321*, 149−156.
62. Miksovska, J., Schiffer, M., Hanson, D. K., and Sebban, P. (1999) *Proc. Natl. Acad. Sci. U.S.A. 96*, 14348−14353.
63. Maróti, P., and Wraight, C. A. (1988) *Biochim. Biophys. Acta 934*, 329−347.
64. Hienerwadel, R., Grzybek, S., Fogel, C., Kreutz, W., Okamura, M. Y., Paddock, M. L., Breton, J., Nabedryk, E., and Mäntele, W. (1995) *Biochemistry 34*, 2832−2843.
65. Nabedryk, E., Breton, J., Hienerwadel, R., Fogel, C., Mäntele, W., Paddock, M. L., and Okamura, M. Y. (1995) *Biochemistry 34*, 14722−14732.
66. Nabedryk, E., Breton, J., Okamura, M. Y., and Paddock, M. L. (1998) *Biochemistry 37*, 14457−14462.
67. Breton, J., Navedryk, E., Mioskowski, C., and Boullais, C. (1996) in *The Reaction Center of Photosynthetic Bacteria—Structure and Dynamics* (Michel-Beyerle, M.-E., Ed.) pp 381−394, Springer, Berlin.
68. Breton, J., and Nabdryk, E. (1998) *Photosynth. Res. 55*, 301−307.
69. Paddock, M. L., Feher, G., and Okamura, M. Y. (1997) *Biochemistry 36*, 14238−14249.
70. Paddock, M. L., Rongey, S. H., Feher, G., and Okamura, M. Y. (1989) *Proc. Natl. Acad. Sci. U.S.A. 86*, 6602−6606.
71. Takahashi, E., and Wraight, C. A. (1992) *Biochemistry 31*, 855−866.
72. Breton, J., Bibikova, M., Oesterhelt, D., and Nabedryk, E. (1999) *Biochemistry 38*, 11541−11552.
73. Kraulis, P. J. (1991) *J. Appl. Crystallogr. 24*, 946−950.

BI000413C